Electrochemical and Solid-State Letters, **11** (7) A119-A124 (2008)
1099-0062/2008/11(7)/A119/6/$23.00 © The Electrochemical Society

Transmission Electron Microscope Studies of $LiNi_{1/3}Mn_{1/3}Co_{1/3}O_2$ before and after Long-Term Aging at 70°C

Heike Gabrisch,[a,*,z] Tanghong Yi,[a] and Rachid Yazami[b,*]

[a]*Advanced Materials Research Institute, University of New Orleans, New Orleans, Louisiana 70148, USA*
[b]*Division of Chemistry and Chemical Engineering, California Institute of Technology, Pasadena, California 91125, USA*

$LiNi_{1/3}Mn_{1/3}Co_{1/3}O_2$ is a potential cathode material for high-power applications in lithium-ion batteries. While cation ordering on a $\sqrt{3} \times \sqrt{3}$ R30° in-plane superlattice was proposed for the layered structure, the experimental data do not fully support this model. Here, we present a systematic electron diffraction study of $LiNi_{1/3}Mn_{1/3}Co_{1/3}O_2$ in the pristine state and after aging. Our results show that a mixture of different phases in the starting material transforms to the O3-type phase and the cubic spinel phase after aging, accompanied by an increase in the percentage of polycrystals.
 [DOI: 10.1149/1.2919713]

Manuscript submitted February 15, 2008; revised manuscript received April 7, 2008. Available electronically May 15, 2008.

$LiNi_{1/3}Mn_{1/3}Co_{1/3}O_2$ is a promising cathode material for high-energy and high-power applications in lithium-ion batteries.[1] Compared to its $LiCoO_2$ and $LiNi_{1/2}Mn_{1/2}O_2$ analogues, it is marked by a high operating voltage and high thermal stability.[2] However, a high irreversible capacity has been reported,[3-5] the origin of which is still unclear, although oxygen evolution may partly account for it.[5,6] Ohzuku, who earlier reported on the synthesis and electrochemistry of the $LiNi_{1/3}Mn_{1/3}Co_{1/3}O_2$ compound, pursued the synthesis of a layered compound isostructural to $LiNiO_2$ and $LiCoO_2$ in which the transition metal (TM) ions exhibit a long-range ordering within the TM layer.[2] Extensive first-principles calculations accompanied the development of $LiNi_{1/3}Mn_{1/3}Co_{1/3}O_2$.[7-9] The results of these calculations show that the in-plane ordered $LiNi_{1/3}Mn_{1/3}Co_{1/3}O_2$ compound is energetically more stable than an assembly of $LiCoO_2$, $LiMnO_2$, and $LiNiO_2$ slabs, while no evidence for a preferred stacking sequence of $LiNi_{1/3}Mn_{1/3}Co_{1/3}O_2$ slabs was found.[9] Element-specific lattice sites for the in-plane positions of cobalt, nickel, and manganese ions are assigned using a $\sqrt{3} \times \sqrt{3}$ R30° superlattice (in Woods notation) which reduces the symmetry of the unit cell from $R\bar{3}m$ in $LiCoO_2$ to $P3_112$ in $LiNi_{1/3}Mn_{1/3}Co_{1/3}O_2$. Energy considerations of the phases in the three binary systems that constitute the ternary system $LiCoO_2$–$LiMnO_2$–$LiNiO_2$ showed that a new phase $LiNi_{0.5}Mn_{0.5}O_2$ forms in the $LiNiO_2$–$LiMnO_2$ system. In comparison, $LiCoO_2$ and $LiNiO_2$ are predicted to form solid solutions, whereas $LiNiO_2$ and $LiMnO_2$ are found to be immiscible.[8] Experimental evidence for in-plane ordering in $LiNi_{1/3}Mn_{1/3}Co_{1/3}O_2$ has been presented in the form of electron diffraction patterns having superlattice reflections corresponding to the $\sqrt{3} \times \sqrt{3}$ R30° unit cell.[10] The authors attribute the weak intensity of the observed superlattice reflections to the small difference in atomic scattering factors of Ni, Mn, and Co and to insufficient long-range ordering. However, a lack of evidence for cation ordering in $LiNi_{1/3}Mn_{1/3}Co_{1/3}O_2$ was found in a recent study of magnetic properties.[11] Crystal structure conversion to spinel upon cycling or thermal treatment has also been reported.[6,12]

The complex interactions between the three TM ions within the oxygen framework of layered $LiNi_{1/3}Mn_{1/3}Co_{1/3}O_2$ are not understood yet, and little literature exists on the details of the initial microstructure and its stability with electrochemical cycling. Here, we present a systematic study of $LiNi_{1/3}Mn_{1/3}Co_{1/3}O_2$ using electron diffraction. We characterize the compound in the as-received state, after thermal aging in the charged state, and after charge to high voltage. Our results indicate that the starting material is inhomogeneous with respect to TM distribution, but adopts to two stable configurations after aging or high-voltage charge.

* Electrochemical Society Active Member.
[z] E-mail: hgabrisc@uno.edu

Experimental

$LiNi_{1/3}Mn_{1/3}Co_{1/3}O_2$ powder prepared according to the method described by Ohzuku et al.[2] was provided by ENAX Co. Japan. The powder was used as the cathode active material in lithium half-cells. The electrolyte consisted of a molar solution of $LiPF_6$ in an equal volume mixture of ethylene carbonate and dimethyl carbonate. Cells were cycled five times between 3 V and 4.5 V. The charge and discharge capacity stabilized at 180 and 175 mAh/g, respectively, in agreement with the literature.[13] After the fifth cycle the cells were charged to 4.5 V and subjected to aging for 60 days at 70°C at the initial charge state at open circuit. Additionally, cells were charged to a high voltage of 5.2 V and maintained at that voltage until the capacity reached 277 mAh/g, corresponding to a full delithiation ($x = 0$ in $Li_xNi_{1/3}Mn_{1/3}Co_{1/3}O_2$). After thermal aging or high-voltage charging, cells were discharged to 3 V and disassembled in an argon atmosphere. The mixture of active material, carbon black, and binder was retrieved from the cathodes. For comparison, powder was retrieved from an uncycled cathode. The powder mixtures were washed repeatedly in *n*-methyl pyrrolidone, followed by a wash in ethanol. The suspension was transferred onto a holey carbon film for transmission electron microscope (TEM) specimen preparation. Electron diffraction studies and dark-field imaging were performed using the JEOL 2010 TEM at the University of New Orleans and the JEOL 3010 at Lawrence Berkeley National Laboratory operated at accelerating voltages of 200 and 120 kV, respectively. Diffraction patterns were obtained from different regions in each particle to investigate the uniformity of the crystal lattice. Experimental electron diffraction patterns were compared to diffraction patterns simulated with the software Electron Microscopist using the following unit cells: layered O3 phase ($R\bar{3}m$ symmetry),[14] cubic spinel phase of compositions $LiTM_2O_4$ (Li in tetrahedral coordination), and $Li_2TM_2O_4$ (Li in octahedral coordination) (space group $Fd\bar{3}m$),[15] in-plane ordering with $\sqrt{3} \times \sqrt{3}$ R30° superlattice (space group $P3_121$),[9] monoclinic (space group $P2/m$).[16]

Results

We analyzed 25 particles of the starting material, 16 aged particles and 17 particles subjected to charge to 5.2 V. In all the samples the majority of diffraction patterns can be indexed completely in the unit cell of the O3 structure. Possible interpretations of O3-type diffraction patterns are given in the Discussion section. A few particles of each sample have reflections typical of the cubic spinel phase located halfway between the fundamental reflections of the O3 phase. In the pristine powder, additional extra reflections of different origin are observed in 46% of the diffraction patterns. They can be classified into three categories, including the $\sqrt{3} \times \sqrt{3}$ R30° in-plane ordered unit cell suggested by Ohzuku. The intensity of the extra reflections varies from faint to strong, indicating fluctuations in the degree of cation ordering. However, for statistical purposes we

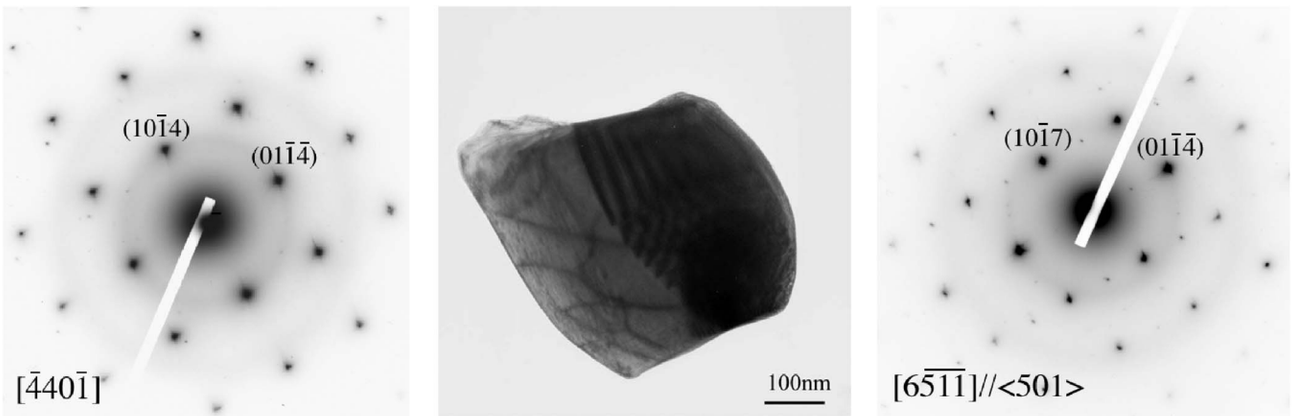

Figure 1. Diffraction patterns of the pristine material. (a) O3-type phase observed in a single crystal. (b) Image of a bicrystal formed by O3-type phase neighboring spinel phase. (c) Diffraction pattern of the crystal appearing dark in (b) showing typical reflections on the cubic spinel phase.

do not distinguish between faint and strong intensity. We count the number of diffraction patterns of each configuration in each cell (starting material, aged, high-voltage discharge), which is higher than the number of particles due to the occurrence of polycrystals. The percentage of patterns with extra reflections other than those due to spinel-type ordering decreases from 46% in the pristine sample to 16% after aging, balanced by an increase in particles having O3 or spinel diffraction patterns. After charge to 5.2 V only O3 and spinel phases are observed. The rearrangement of cations during aging is accompanied by changes in particle morphology. The fraction of bi- and tricrystals in the starting material and in particles subjected to high voltage is comparable at values of 16% and 18%, respectively. After aging in the charged state, about 44% of the analyzed particles are polycrystals.

Pristine $LiNi_{1/3}Mn_{1/3}Co_{1/3}O_2$ powder.— Out of 25 particles analyzed, 21 show uniform diffraction patterns across single-crystalline particles or across the grains in a polycrystalline particle. The polycrystalline particles include one bicrystal that is part O3 and part spinel phase separated by a grain boundary, and one tricrystal formed by three O3 crystals having a well-defined orientation relationship. The diffraction patterns of these 21 particles can be classified into five categories. (*i*) Diffraction patterns indexed completely as O3 phase (Fig. 1a). (*ii*) Diffraction patterns with $\{10\bar{1}0\}$ reflections that are forbidden in the O3 structure (Fig. 2a). (*iii*) Diffraction patterns with superlattice reflections corresponding to the $\sqrt{3} \times \sqrt{3}$ R30° superlattice (Fig. 2b). (*iv*) Diffraction patterns with sets of three extra diffraction spots halfway between fundamental $\{11\bar{2}0\}$ or $\{1\bar{1}01\}$ reflections. The spacing between the extra spots is $d/6$ (d = distance between two fundamental reflections), suggesting that a full set of these reflections consists of five spots. In all observed cases only three reflections are present. We call this configuration "triplet;" see Fig. 3b and c. (*v*) Diffraction patterns representative of the cubic spinel phase with extra reflections halfway between the fundamental diffraction spots. An example of the spinel phase adjacent to pure O3-type phase in a bicrystal is shown in Fig. 1b and c.

The patterns obtained from the remaining four particles showed variations in the cation distribution across each particle that cannot be clearly associated with distinct crystals. These particles are classified as multiple pattern particles in Table I. Two particles have diffraction patterns representative of the $\sqrt{3} \times \sqrt{3}$ R30° ordering throughout the crystal; additionally, forbidden $\{10\bar{1}0\}$ reflections (particle 1) or triplets (particle 2) are superimposed in some regions of the particle. From image contrast a boundary between two crystals can be distinguished in particle 1 while particle 2 appears to be a single crystal. In two different particles, variations in the diffraction patterns are observed that can be classified as neighboring regions of O3: (*i*) triplets between $\{11\bar{2}0\}$ and $\{1\bar{1}01\}$ reflections, and spinel (particle 3), and (*ii*) spinel, $\sqrt{3} \times \sqrt{3}$ R30° ordering and triplets (particle 4). Particle 3 appears to be a tricrystal but exhibits five

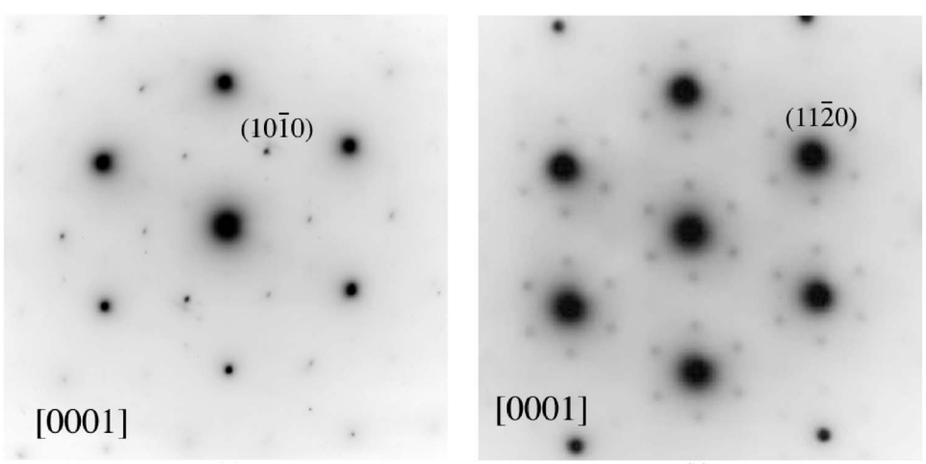

Figure 2. Diffraction patterns representative of two types of cation arrangement. (a) Appearance of forbidden $\{10\bar{1}0\}$ reflections. (b) Superlattice reflections typical of a $\sqrt{3} \times \sqrt{3}$ R30° in-plane ordering.

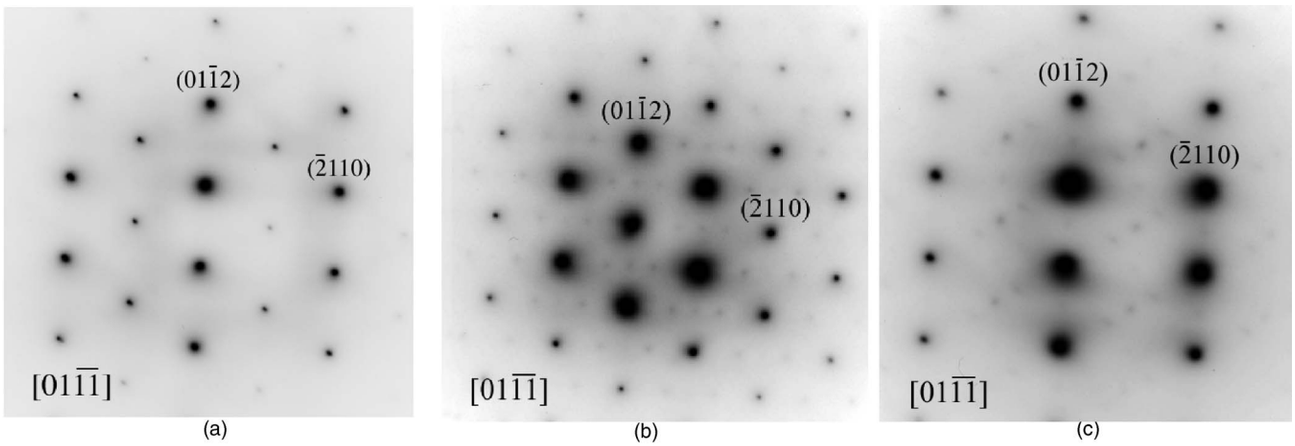

Figure 3. Three diffraction patterns taken from neighboring regions of a pristine particle. (a) Pattern representative of O3 phase seen along the $[01\bar{1}\bar{1}]$ zone axis direction. (b) Pattern in same zone axis direction having additional reflections (triplets) between $(\bar{2}110)$ diffractions. (c) Pattern in same specimen orientation with weakened intensity at positions of (1101) diffractions; instead, triplets between (2202) reflections have appeared.

types of diffraction patterns. In particle 4 no distinct crystals can be recognized. Out of the 25 analyzed particles, 4 are clearly identified as polycrystals (16% of the analyzed particles), while the classification for particles 2 and 4 is not clear. The analysis results obtained from all patterns of the pristine powder are summarized in Table I.

Thermally aged and overcharged $LiNi_{1/3}Mn_{1/3}Co_{1/3}O_2$ *powders.*— The main diffraction types observed after aging are O3, spinel, and forbidden $\{10\bar{1}0\}$ reflections. In one case the forbidden $\{10\bar{1}0\}$ reflections are superimposed with very faint reflections of the $\sqrt{3} \times \sqrt{3}$ R30° in-plane ordering. Compared to the starting material, the fraction of polycrystals has increased from 4 out of 25 (starting material) to 6 out of 16 (or 44%) after aging. The cubic spinel phase is most often found in bicrystals neighboring O3-type crystals. An example is given in Fig. 4a-c, where the spinel phase appears bright in the imaging condition used here [dark-field imaging with $(\bar{1}11)$ of the cubic spinel phase, Fig. 4b]. The oxygen lattice of the two crystals is aligned parallel, resulting in the orientation relationship $(0001)//\{111\}$ and $[1\bar{1}00]//\langle 110\rangle$, diffraction patterns of O3 and spinel shown in Fig. 4a and c. Other bicrystals and tricrystals could be indexed completely as O3 phase (3 out of 7 polycrystals). An example showing a particle composed of two O3 crystallites rotated about 180° with respect to each other is given in Fig. 5. The diffraction patterns in Fig. 5a and b are taken from the areas marked by A and B in the image of the particle shown in Fig. 5d. The superposition of the two patterns forms the diffraction pat-

Table I. Classification of diffractions patterns obtained of 25 pristine particles.

Diffraction type	Number of diffraction patterns		Comments
O3	15	43%	Including one O3 tricrystal, 1 bicrystal, part spinel 1 in multiple pattern particles
$\sqrt{3} \times \sqrt{3}$ R30°	7	20%	Including 3 in multiple pattern particles
Triplets	6	17%	Including 3 in multiple pattern particles
Forbidden $\{10\bar{1}0\}$	3	9%	Including 2 in multiple pattern particles
Spinel	4	11%	1 bicrystal, part pure O3 2 in multiple pattern particles

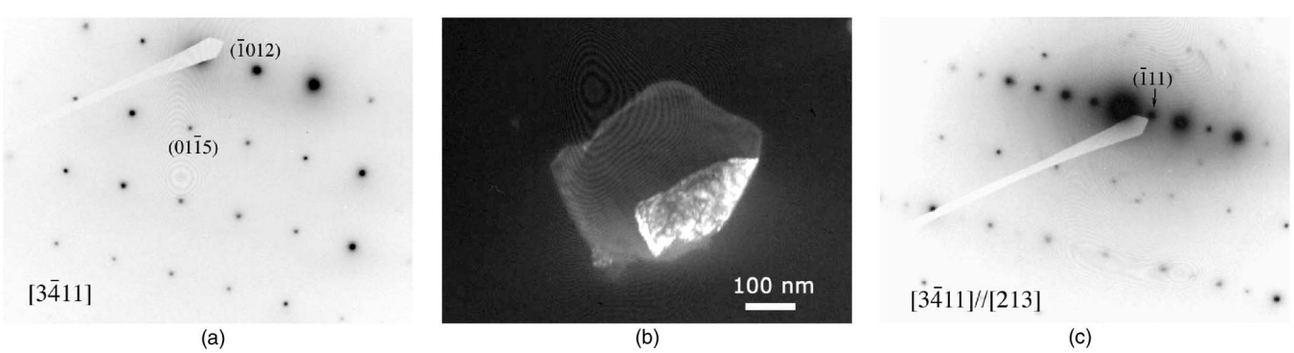

Figure 4. Diffraction patterns and image of an O3/spinel bicrystal taken from the aged cathode. (a) Diffraction pattern indexed completely as O3 phase. (b) Dark-field image taken with a $(\bar{1}11)$ reflection of the cubic spinel phase. (c) Diffraction pattern of the cubic spinel phase.

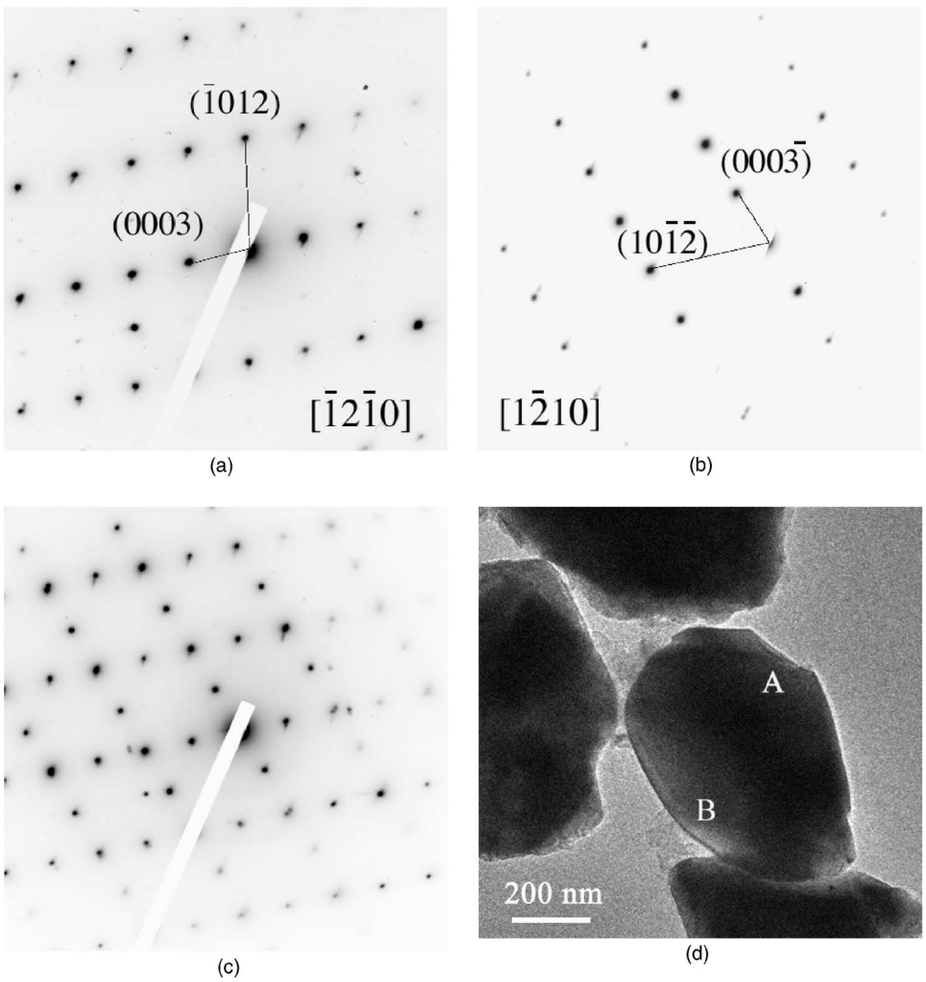

Figure 5. Bicrystal formed by two O3 crystallites, twinned in the (0001) plane. (a), (b) Diffraction patterns of regions A and B marked in the image of the particle shown in (d). (c) Shows a diffraction pattern of the whole particle where the contributions of (a) and (b) superimpose.

tern of the whole particle, which is shown in Fig. 5c. Analysis shows that the particle twinned in the (0001) plane. Similar configurations were observed in the starting material, however at a much lower rate (1 out of 25 analyzed particles compared to 3 out of 16 in the aged sample).

After charge to high voltage, only patterns of the O3 phase and of the spinel phase were observed. We observed streaking of (0003) reflections in some O3 patterns, accompanied by contrast variations in the image parallel to (0001) planes. Spinel-type reflections are very weak and are found either in single crystals or in bicrystals adjacent to a crystal of O3 phase (two bicrystals). Of the 17 analyzed particles, 3 were polycrystals (18%).

A summary of the analyses of particles retrieved from the aged cell and of the cell charged to high voltage is given in Table II.

Table II. Classification of analyzed particles retrieved from the aged cell (16 particles) and the cell charged to high voltage (17 particles).

Diffraction type	Number of patterns		Remarks
	Particles retrieved from aged half-cell		
O3	17	68%	Including 3 polycrystals of pure O3-type
Forbidden $\{10\bar{1}0\}$	3	12%	1 superimposed with a $\sqrt{3} \times \sqrt{3}$ in bicrystal (part O3)
$\sqrt{3} \times \sqrt{3}$ R30°	1	4%	Weak $\sqrt{3} \times \sqrt{3}$ ordering, superimposed to forbidden $\{10\bar{1}0\}$
Spinel	4	16%	3 bicrystals (O3 and spinel in separate regions)
	Particles retrieved from cell charged to 5.2 V		
O3	15	75%	1 O3 bicrystal
Spinel	5	25%	2 bicrystals part spinel (very faint spinel intensity)

Discussion

To our knowledge this is the first systematic electron diffraction study of crystal structures observed in pristine and cycled $LiNi_{1/3}Mn_{1/3}Co_{1/3}O_2$. In earlier reports electron diffraction patterns typical for the in-plane $\sqrt{3} \times \sqrt{3}$ R30° unit cell in $LiNi_{1/3}Mn_{1/3}Co_{1/3}O_2$ were presented, however, without mentioning the frequency with which the superlattice had been observed.[10] Furthermore, the weak intensity of superlattice reflections in Ref. 10 is partly attributed to insufficient long-range ordering, indicating that the successful synthesis of an ordered $LiNi_{1/3}Mn_{1/3}Co_{1/3}O_2$ compound is not straightforward, possibly questioning the predicted stability of the ordered compound. Strong superlattice reflections typical of the $\sqrt{3} \times \sqrt{3}$ R30° superlattice are observed in $LiNi_{0.5}Mn_{0.5}O_2$ when a third species is introduced into the TM layer through interlayer mixing between Li and Ni ions.[17,18] $LiNi_{0.5}Mn_{0.5}O_2$ produced by ion exchange where interlayer mixing is suppressed does not exhibit long-range ordering.[19] In our study, both weak and strong $\sqrt{3} \times \sqrt{3}$ R30° superlattice reflections were observed, but at a low frequency of only about 20% of particles in pristine $LiNi_{1/3}Mn_{1/3}Co_{1/3}O_2$ powder. After aging and overcharge to 5.2 V, this number decreases to 7 and 0%, respectively. Similarly, the "triplets" and forbidden $\{10\bar{1}0\}$ reflections observed in the pristine material disappear after aging or overcharge. In the literature we find information that supports the stability of the ordered phase as well as data that point to a random cation distribution in $LiNi_{1/3}Mn_{1/3}Co_{1/3}O_2$. Measurements of magnetic properties in $LiNi_{0.5}Mn_{0.5}O_2$ and $LiNi_{1/3}Mn_{1/3}Co_{1/3}O_2$ provide no evidence for ordering in $LiNi_{1/3}Mn_{1/3}Co_{1/3}O_2$, while the experimental results provide evidence for the formation of magnetic clusters in $LiNi_{0.5}Mn_{0.5}O_2$.[11] First-principles calculations seem to support the stability of the ordered phase.[9] These calculations consider ordered $LiNi_{1/3}Mn_{1/3}Co_{1/3}O_2$ slabs and separate slabs of $LiTMO_2$ (TM = Mn, Co, or Ni); however, no comparison to a random TM distribution is presented. Our experimental findings show that the $\sqrt{3} \times \sqrt{3}$ R30° superlattice reflections disappear after aging or overcharge. A possible explanation for the disappearance of superlattice diffractions is instability of the ordered unit cell, because it has been observed to some extent in the pristine material but to a much lesser extent after cycling. One could argue that changes in the oxidation state of Ni and Co that persist after discharge may lead to the positional rearrangement of oxygen ions that affect the diffracted intensities. At this point our data do not allow us to conclude on the stability of the superlattice in $LiNi_{1/3}Mn_{1/3}Co_{1/3}O_2$.

"Triplets" are found in the starting material only, but disappear after aging or overcharge, suggesting that the underlying cation arrangement is not energetically favored. Similar diffraction patterns were observed in $LiNi_{0.5}Mn_{0.5}O_2$ produced by ion exchange; however, in these studies the extra reflections appear after Li/Ni interchange has been thermally activated through heating to 600°C.[19] The spacing between extra reflections is 1/6 of the distance between {111}-type reflection, identical to our observations ($\{111\}$ is equivalent to $\{11\bar{2}1\}$ in the four-index system). And, comparable to our case, two reflections out of five are systematically missing. In Ref. 19 the reduced spacing between the new reflections is explained by a flower structure formed by Li, Ni, and Mn ions in the TM layer having a unit cell of the size $2 \times \sqrt{3} \times \sqrt{3}$ R30° (doubled superlattice unit cell). The systematic extinction of two out of five reflections is attributed to an undisclosed stacking sequence of the flower structure. In our case the triplets appear between $\{11\bar{2}0\}$ and $\{1\bar{1}01\}$ fundamental reflections, where triplets between $\{1\bar{1}01\}$ reflections are not in agreement with a $2\sqrt{3} \times \sqrt{3}$ R30° in-plane unit cell. The triplets between $\{11\bar{2}0\}$ and $\{1\bar{1}01\}$ reflections are observed in the same crystal, indicating a continuous change in the cation arrangement. We did not attempt to model possible cation distributions that could explain the observed triplets.

The appearance of forbidden $\{1\bar{1}00\}$ reflections in the starting material indicates that the rhombohedral symmetry of the $R\bar{3}m$ unit cell has been destroyed. Microstructural features that have the potential to break the "R" symmetry include stacking fault formation, staging of Li ions as modeled in Ref. 20, shift of oxygen from its ideal positions, or exchange of TM ions and Li between their respective layers. In the O2 and the O1 phases of $LiCoO_2$ that do not belong to the group of rhombohedral systems $\{1\bar{1}00\}$ diffractions are allowed. The tendency of nickel ions to interchange positions with lithium ions is well known.[21,22] Simulated electron diffraction patterns using a modified unit cell of the O3 unit cell in which one Li and 1 Ni atom are exchanged show that this interchange can give rise to diffracted intensity at the positions of forbidden $\{1\bar{1}00\}$ reflections. However, alternative arrangements cannot be excluded based on the data at hand. Therefore, additional experiments (e.g., Rietveld refinement of powder diffraction data) are required for an unambiguous interpretation of the observed forbidden reflections. We find diffraction patterns with forbidden $\{1\bar{1}00\}$ reflections in the starting material, and to some extent after aging, but not after charge to high voltage. A similar observation was reported by Li et al., who studied $LiNi_{0.5}Mn_{0.5}O_2$ before and after charge to 5.3 V.[23] In the pristine material about 95% of particles showed the $\sqrt{3} \times \sqrt{3}$ R30° superlattice reflections, which the authors interpret as a consequence of Li/Ni interchange. This percentage decreased to 19% after overcharge. From the combined results of electron diffraction and synchrotron X-ray powder diffraction on pristine and charged powders, the authors conclude that upon charge Ni migrates from the Li layer into the TM layer, thus reversing the Li/Ni interchange.

The observation of an increased fraction of polycrystals in the aged specimen adds an important detail to the understanding of microstructural processes in $LiNi_{1/3}Mn_{1/3}Co_{1/3}O_2$. Compared to the pristine powder, the fraction of polycrystals has roughly doubled in the aged sample, where sufficient time and thermal activation energy for diffusion-controlled processes was available. At the same time we also find an increase of the spinel phase after aging that can only be formed when a sufficient number of TM ions move to the Li layer. The polycrystals in all samples can be indexed either as pure O3 phase or as part O3 and part spinel phase. The nature of the cubic spinel phase (composition, Li positions in tetrahedral or octahedral coordination) cannot be determined by this investigation because Li in tetrahedral or octahedral coordination merely leads to variations in the intensity of spinel-type reflections. Diffracted intensity, however, depends on several factors that have not been controlled in this investigation. Therefore, we cannot distinguish between different Li coordinations or compositions based on electron diffraction patterns here. It is reasonable to assume that the spinel phase in the pristine material has the composition $Li_2TM_2O_4$ (octahedral coordination of Li), whereas the spinel phase in the sample retrieved from the aged cathode is likely to have the composition $LiTM_2O_4$.[24] We report large variations in the intensity of spinel diffractions indicative of different degrees of cation ordering. Nevertheless, the clear separation of two grains in one particle by dark-field imaging as shown in Fig. 4 is evidence for the presence of two phases with different cation ordering. In a first approximation, diffraction patterns indexed as O3 phase may be the result of random placement of TM ions on the 3*a* sites in the $R\bar{3}m$ structure leading to an average atomic scattering factor. Alternatively, one could speculate that different TM species segregate into separate regions of a particle driven by the predicted immiscibility of Co and Mn in $LiTMO_2$ or by the tendency of Mn and Ni to form the separate phase $LiMn_{0.5}Ni_{0.5}O_2$.[8] To distinguish between these two models, an elemental analysis of different regions within a particle is required. At present we conclude that growth processes accompany the rearrangement of cations during aging. Support for this conclusion can be found in the comparison of shape and length of two grain boundaries observed in a pristine and in an aged particle; see Fig. 1 and 4, respectively. In Fig. 4a the grain boundary between the spinel and O3 phase in an aged particle bulges out from the spinel into the O3 phase as if the particle was interrupted in an ongoing transformation

process. This grain boundary does not take on the shortest possible length required by energy considerations. For comparison, the grain boundary between the spinel and O3 phase in a pristine particle in Fig. 1c is in a low-energy configuration, adapting to the shortest possible length. More studies by dark-field imaging are required to confirm the theory of grain boundary movement during aging.

A comparison between microstructures observed in $LiCoO_2$ and in $LiNi_{1/3}Mn_{1/3}Co_{1/3}O_2$ subjected to aging shows that, in the former, the spinel phase forms on the particle surface, while in $LiNi_{1/3}Mn_{1/3}Co_{1/3}O_2$ the spinel occupies large fractions of a particle's volume.[24]

Conclusions

$LiNi_{1/3}Mn_{1/3}Co_{1/3}O_2$ investigated in this study has an inhomogeneous cation distribution in the as-synthesized state that converts to a mixture of particles having O3 and spinel structure after aging or charge to high voltage. Only a small percentage of particles showed typical diffractions of the in-plane ordering in a $\sqrt{3} \times \sqrt{3}$ R30° supercell initially. We speculate that the degree of inhomogeneity in the pristine material may vary according to the powder preparation method and conditions. In fact, the reported oxygen loss[5,6] may trigger cation rearrangement inside and outside the TM layer to account for the local charge compensation.

The substantially increased number of bicrystals after aging compared to the initial state indicates that growth processes accompany cation rearrangement when sufficient time and thermal activation are available. Based on the predicted phases in the binary $LiTM_1TM_2O_2$ systems ($TM_{1,2}$ = Mn, Co, Ni), the interpretation of the observed O3 diffraction patterns is not unambiguous. Additional information on the chemical composition is required, especially in the aged sample, underlining that the interpretation of electron diffraction patterns in complex systems is a delicate undertaking that should be accompanied by spectroscopic techniques to correlate diffraction information to the elemental analysis.

Acknowledgments

This work is supported by the Louisiana Board of Regents under contract no. LEQSF(2007012)-ENH-PKSFI-PRS-04. We thank Enax, Japan, for providing the $Li(Ni_{1/3}Co_{1/3}Mn_{1/3})O_2$ powder.

University of New Orleans assisted in meeting the publication costs of this article.

References

1. I. Belharouak, Y. K. Sun, J. Liu, and K. Amine, *J. Power Sources*, **123**, 247 (2003).
2. T. Ohzuku and Y. Makimura, *Chem. Lett.*, **7**, 642 (2001).
3. K. M. Shaju, G. V. Subba Rao, and B. V. R. Chowdari, *Electrochim. Acta*, **48**, 145 (2002).
4. B. J. Hwang, Y. W. Tsai, D. Carlier, and G. Ceder, *Chem. Mater.*, **15**, 3676 (2003).
5. J. Li, Z. R. Zhang, X. J. Guo, and Y. Yang, *Solid State Ionics*, **177**, 1509 (2006).
6. I. Belharouak, W. Lu, D. Vissers, and K. Amine, *Electrochem. Commun.*, **8**, 329 (2006).
7. Y. Koyama, I. Tanaka, H. Adachi, Y. Makimura, and T. Ohzuku, *J. Power Sources*, **119–121**, 644 (2003).
8. Y. Koyama, Y. Makimura, I. Tanaka, H. Adachi, and T. Ohzuku, *J. Electrochem. Soc.*, **151**, A1499 (2004).
9. Y. Koyama, N. Yabuuchi, I. Tanaka, H. Adachi, and T. Ohzuku, *J. Electrochem. Soc.*, **151**, A1545 (2004).
10. N. Yabuuchi, Y. Koyama, N. Nakayama, and T. Ohzuku, *J. Electrochem. Soc.*, **152**, A1434 (2005).
11. N. A. Chernova, M. Ma, J. Xiao, M. S. Whittingham, J. Breger, and C. P. Grey, *Chem. Mater.*, **19**, 4682 (2007).
12. S. H. Park, C. S. Yoon, S. G. Kang, H.-S. Kim, S.-I. Moon, and Y.-K. Sun, *Electrochim. Acta*, **49**, 557 (2004).
13. N. Yabuuchi, Y. Makimura, and T. Ohzuku, *J. Electrochem. Soc.*, **154**, A314 (2007).
14. J. Akimoto, Y. Gotoh, and Y. Oosawa, *J. Solid State Chem.*, **141**, 298 (1998).
15. R. J. Gummow, D. C. Liles, and M. M. Thackeray, *Mater. Res. Bull.*, **28**, 1177 (1993).
16. Y. Shao-Horn, S. Levasseur, F. Weill, and C. Delmas, *J. Electrochem. Soc.*, **150**, A366 (2003).
17. T. Ohzuku and Y. Makimura, Abstract 1079, The Electrochemical Society Meeting Abstracts, Vol. 2003-1, Paris, France, April 27–May 2, 2003.
18. Y. S. Meng, G. Ceder, C. P. Grey, W.-S. Yoon, and Y. Shao-Horn, *Electrochem. Solid-State Lett.*, **7**, A155 (2004).
19. Y. Hinuma, Y. S. Meng, K. Kang, and G. Ceder, *Chem. Mater.*, **19**, 1790 (2007).
20. K. Pruessner, H. Gabrisch, and R. Yazami, Paper 279 presented at The Electrochemical Society Meeting, Honolulu, HI, Oct. 3–8, 2004.
21. W.-S. Yoon, S. Iannopollo, C. P. Grey, D. Carlier, J. Gorman, J. Reed, and G. Ceder, *Electrochem. Solid-State Lett.*, **7**, A167 (2004).
22. P. S. Whitfield, I. J. Davidson, L. M. D. Cranswick, I. P. Swainson, and P. W. Stephens, *Solid State Ionics*, **176**, 463 (2005).
23. H. H. Li, N. Yabuuchi, Y. S. Meng, S. Kumar, J. Breger, C. P. Grey, and Y. Shao-Horn, *Chem. Mater.*, **19**, 2551 (2007).
24. H. Gabrisch, R. Yazami, and B. Fultz, *J. Electrochem. Soc.*, **151**, A891 (2004).